



RESEARCH PAPER

 OPEN ACCESS 

## Role of circRNA circ\_0000080 in myocardial hypoxia injury

Bo Wang, Yuyang Zhang, Shunmiao Fang, and Hui Wang

Department of Cardiology, Xi'an City, Shaanxi Province, China

### ABSTRACT

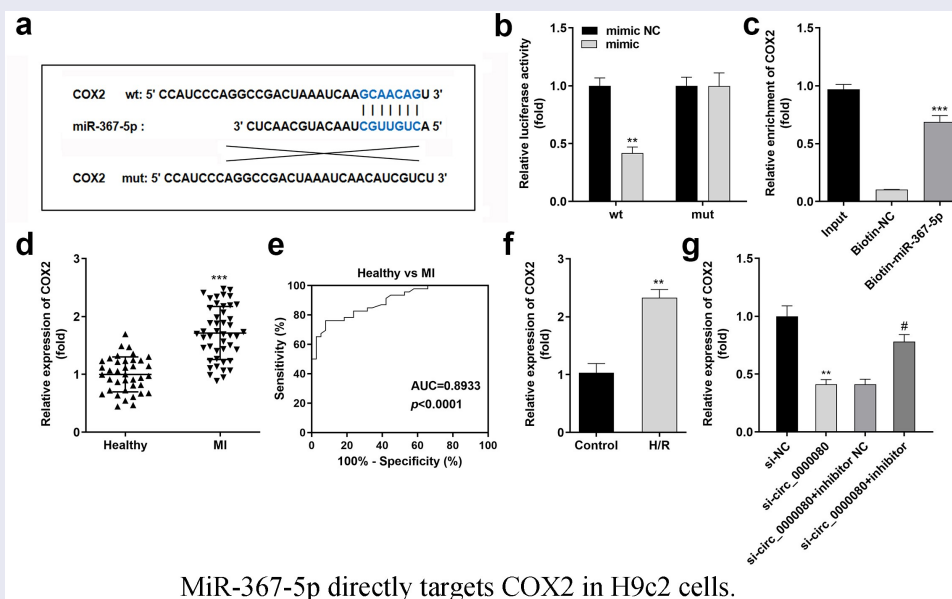
This study aimed to investigate the potential role of circRNA circ\_0000080 in myocardial hypoxia injury and the underlying mechanisms. Patients with myocardial hypoxia injury who were admitted to Xi'an No. 1 Hospital, China, were included in this study. The expression levels of circ\_0000080, miR-367-5p, and COX2 were analyzed by real-time quantitative PCR (RT-qPCR); cell viability was measured by cell counting kit-8 (CCK-8) assay; and apoptosis was detected by flow cytometry. In addition, the release of cytokines was determined by Enzyme-linked immunosorbent assay (ELISA), and the binding sites between miR-367-5p and circ\_0000080/COX2 were predicted by bioinformatics analysis and confirmed by dual-luciferase reporter and RNA pull-down assays. circ\_0000080 was upregulated in patients with MI and in H9c2 cells treated with H<sub>2</sub>O<sub>2</sub> and hypoxia/reoxygenation (H/R). Silencing circ\_0000080 reduced the H/R-mediated apoptosis of cardiomyocytes and secretion of pro-inflammatory cytokines. Moreover, circ\_0000080 functioned as an miR-367-5p sponge to regulate the expression of COX2. Downregulated miR-367-5p or overexpressed COX2 degraded cellular functions of cardiomyocytes. circ\_0000080 knockdown alleviated myocardial hypoxia injury through the miR-367-5p/COX2 axis.

### ARTICLE HISTORY

Received 4 January 2022  
Revised 6 April 2022  
Accepted 8 April 2022

### KEYWORDS

Circ\_0000080; miR-367-5p; COX2; myocardial hypoxia injury






### Highlights

- circ\_0000080 is upregulated in patients with MI and in H/R-treated cells.
- MiR-367-5p is a target of circ\_0000080.
- MiR-367-5p knockdown reverses the effect of circ\_0000080.

### Introduction

Myocardial infarction (MI) is an ischemic cardiomyopathy with high morbidity and mortality, with high global prevalence [1,2]. Myocardial apoptosis induced by oxidative stress can be caused by the sudden and persistent interruption of cardiac blood supply during

**CONTACT** Hui Wang  [wanghui0501@qq.com](mailto:wanghui0501@qq.com)  Department of Cardiology, Xi'an No. 1 Hospital, No. 30, Fenxiang, South Main Street, Xi'an City, Shaanxi Province 710002, China

 Supplemental data for this article can be accessed [here](#)

© 2022 The Author(s). Published by Informa UK Limited, trading as Taylor & Francis Group.

This is an Open Access article distributed under the terms of the Creative Commons Attribution License (<http://creativecommons.org/licenses/by/4.0/>), which permits unrestricted use, distribution, and reproduction in any medium, provided the original work is properly cited.

MI, superoxide overload, and disruption of calcium homeostasis after reperfusion therapy [3,4]. Following apoptosis, myocardial cells are replaced by fibroblasts, leading to systolic dysfunction of the left ventricle and eventually the induction of heart failure [5]. Therefore, uncovering the molecular mechanism underlying myocardial cells is of great importance in the treatment of MI.

Compared to traditional linear RNA, circRNA, with a closed circular structure, is more stable [6,7]. Circular RNAs play critical roles in physiological and pathological processes, and they are involved in the occurrence and development of many diseases, such as cardiovascular diseases [8,9]. Researchers have highlighted the role of circRNA in MI and suggested that the regulation of circFndc3b expression may promote the recovery and remodeling of cardiac function after MI [10]. circMAP3K5 is a major regulator of TET2-mediated SMC differentiation in intimal hyperplasia, as observed in restenosis and atherosclerosis [11]. By inhibiting miR-26b-5p and miR-140-3p, circRNA\_000203 may increase GATA4 level and exacerbate cardiac hypertrophy [12]. However, the role of circ\_0000080 in cardiomyocyte apoptosis remains unclear.

MicroRNAs are a class of non-coding single-stranded RNA, approximately 21–23 nucleotides long [13,14]. MiR-367-5p is related to cell growth and proliferation; it participates in the occurrence and development of gastric cancer, mandibular protrusion, and other related diseases, and it is important for their diagnosis and treatment [15,16]. To date, the role and mechanism of miR-367-5p in MI remain elusive.

Here, we aimed to reveal the protective effect of circ\_0000080 on oxidative stress injury in myocardial cells induced by hypoxia/reoxygenation. We try to elucidate the effect of circ\_0000080/miR-367-5p/COX2 axis on myocardial viability, apoptosis, and inflammation. Overall, this study provides an important theoretical basis for the development of therapeutic targets for treating MI.

## Methods

### *Patients and clinical specimen*

A total of 38 healthy heart tissues and 45 heart tissues from patients with MI were obtained.

The human heart tissue samples were obtained from patients with their consent and their use for research was approved by the ethical review board of Xi'an No. 1 Hospital (ethics number: 2021JM-587).

### *Cell culture*

Rat embryonic cardiomyocyte H9c2 was purchased from Shanghai Cell Bank of Chinese Academy of Sciences (Shanghai, China). The cells were cultured in Dulbecco's modified Eagle medium (DMEM) in an incubator at 37°C, with saturated humidity and 5% CO<sub>2</sub>.

### *Construction of the myocardial ischemia-reperfusion injury cell model*

When the growth density of H9C<sub>2</sub> cells exceeded 90%, the supernatant of the culture medium was replaced by DMEM without fetal bovine serum. Thereafter, H9c2 cells were placed in an incubator (5% CO<sub>2</sub> and 95% N<sub>2</sub>) for 4 h, and then cultured in DMEM containing 10% glycerol (5% CO<sub>2</sub> and 95% O<sub>2</sub>) for 3 h, followed by 24 h of oxygen.

### *Cell transfection*

Cardiomyocytes were seeded in a 6-well plate. According to the operating instructions, transfection was performed when the degree of cell fusion exceeded 60%. Briefly, Lipofectamine 2000 and plasmid were diluted in Opti-MEM, respectively. After 5 min, the diluted Lipofectamine 2000 and plasmid were mixed evenly. The transfection complex was then added to the 6-well plate and replaced with fresh medium after 4–6 h of transfection. The transfection plasmid used in this study was constructed by Tsingke Biotechnology (Guangzhou, China). SiRNA was transfected with Lipofectamine 2000. The sequences of siRNAs were as follows: si-NC: 5'-AGTGGGTCTACGGCGATA-3', si-circ\_0000080 1#: 5'-GTTTGGAGGAACTCAACCCTA-3', and si-circ\_0000080 2#: 5'-TTTGGAGGAACTCAACCCTAT-3'.

### Real-time quantitative PCR (qRT-PCR)

For fluorescent probe PCR, the following components were added to a 20  $\mu$ L PCR mixture (catalog No. 4,369,016; ABI, USA): 10  $\mu$ L TaqMan Gene Expression PCR Master Mix, 1  $\mu$ L template DNA, 1  $\mu$ L 20 $\times$  Prime Probe mixture, 8  $\mu$ L DNase-free water, and 9.4  $\mu$ L DNase-free water. The following cycling conditions were used for PCR: 95°C 10 min; 95°C 15s, 60°C 30s, 68°C 30s, 40 cycles. Using the internal reference gene, *GAPDH*, as a reference, the relative content of the target sample gene was calculated. Commercial TaqMan primers for qPCR were purchased from Life Technologies, USA. The primers were: circ\_0000080 F: 5'-GAGGAACACTCCATATAAT TGGTGA-3'; R: 5'-TCTGTTTTTCTTTGAAGG GCTACCT-3', miR-367-5p F: 5'-TGCGGACTGT TGCTAATATG-3'; R: 5'-CCAGTGCAGGGTCC GAGGT-3', COX2 F: 5'-TTCAAATGAGATTGTG GGAAAAT-3'; R: 5'-AGATCATCTCTGCCTGAG TATCTT-3'.

### Cell counting kit-8 (CCK-8) assay

After H9c2 cells were transfected as indicated and treated with hypoxia/reoxygenation (H/R), 10  $\mu$ L CCK-8 (Catalog No. C0037; Beyotime, Shanghai, China) was added to each well. After 2 h, the absorbance of each sample was measured at 450 nm according to the kit instruction.

### Apoptosis analysis

Flow cytometry was performed according to a previous study [17]. After H9c2 cells were transfected as indicated and treated with H/R, an (annexin V + PI) apoptosis detection kit (Catalog No. C1062L; Beyotime) was used for quantitative analysis by flow cytometry.

### Western blot

Cells were lysed using RIPA buffer. After detecting protein concentration using BCA kit (Catalog No. P0010; Beyotime), equal protein was added and run on 10% SDS-PAGE. Then the protein was transferring to PVDF membranes, followed by blocked with 5% skim milk for 1 h. The

membranes were incubated with primary antibodies (anti-Bcl-2: catalog No. ab32124; dilution 1:1000, anti-Bax: catalog No. ab32503; dilution 1:5000, anti-GAPDH: catalog No. ab9485; dilution 1:2500) overnight at 4°C, and incubated with secondary antibody [Goat Anti-Rabbit IgG H&L (HRP): catalog No. ab6721; dilution 1:3000] at room temperature for 1 h. The bands were visualized using ECL plus (Catalog No. P0018M; Beyotime). The original bands were provided in supplemental material 1.

### Enzyme-linked immunosorbent assay (ELISA)

After H9c2 cells were transfected as indicated and treated with H/R, the cell culture supernatant was collected and the concentrations of IL-6, TNF- $\alpha$ , and IL-1 $\beta$  were detected according to the instructions of commercial kits (IL-6 catalog No. 4355; TNF- $\alpha$  catalog No. 920; IL-1 $\beta$  catalog No. 3748; MEIMIAN; Jiangsu, China). ELISA was performed as previous described [18].

### Dual luciferase reporter gene experiment

Target genes were predicted by Starbase v3.0. PMIR-circ\_0000080-wt was formed by cloning circ\_0000080 cDNA into the pMIR-Vector; pMIR-circ\_0000080-mut was inserted by the mutant circ\_0000080. The cloned sequences were provided in supplemental material 2. Similarly, pMIR-COX2-wt or pMIR-COX2-mut was inserted by COX2 cDNA or mutant COX2. When the growth density of H9C<sub>2</sub> cells exceeded 90%, cells were cultured and co-transfected with pMIR-circ\_0000080-wt or pMIR-COX2-wt, pMIR-circ\_0000080-mut or pMIR-COX2-mut, miR-367-5p mimics, and miR-NC, respectively. After 48 h, luciferase was detected with the dual-luciferase reporter gene assay system (catalog No. TM040; Promega, USA) as instructed.

### RNA pull-down assay

The interaction between circ\_0000080 and miR-367-5p or the interaction between miR-367-5p and COX2 in cells was determined by an RNA pull-down assay [17]. Biotin labeled miR-367-5p and biotin-NC were transfected into cells for 72 h. The

transfected cells were lysed using cell lysis buffer. Partial split product was used as the input group, and the others were incubated with M-280 streptavidin magnetic beads (catalog No. 11206D; Sigma-Aldrich, USA) at 4°C for 3 h. After washing in low-salt buffer and high-salt buffer, the expression of circ\_0000080 and COX2 was measured using qRT-PCR.

### Statistical analysis

SPSS 25.0 statistical software was used for data analysis, and the data are expressed as mean  $\pm$  SEM. One-way ANOVA was used for comparison among multiple groups, and the LSD test was used for pairwise comparison.  $P < 0.05$  was considered statistically significant.

### Results

In this study, we sought to explore the expression of circ\_0000080 in MI and its role in H/R-treated

H9c2 cells. We analyzed the effects of circ\_0000080 on cell viability, apoptosis, and inflammation. The goal of this study is to provide an important theoretical basis for the development of therapeutic targets for treating MI.

### Circ\_0000080 is upregulated in MI and H/R-treated H9c2 cells

This experiment was conducted to detect the expression level of circ\_0000080 between MI patients and healthy individuals (controls) to understand the role of circ\_0000080 in the heart. The qRT-PCR results revealed that the expression level of circ\_0000080 was significantly elevated in MI patients than in healthy individuals (Figure 1(a)). The corresponding AUC value of circ\_0000080 for distinguishing between MI patients and healthy controls was 0.9631 (Figure 1(b)). The information of circ\_0000080 was shown in Figure 1(c). Hypoxia/reoxygenation (H/R) treatment increased the circ\_0000080 level

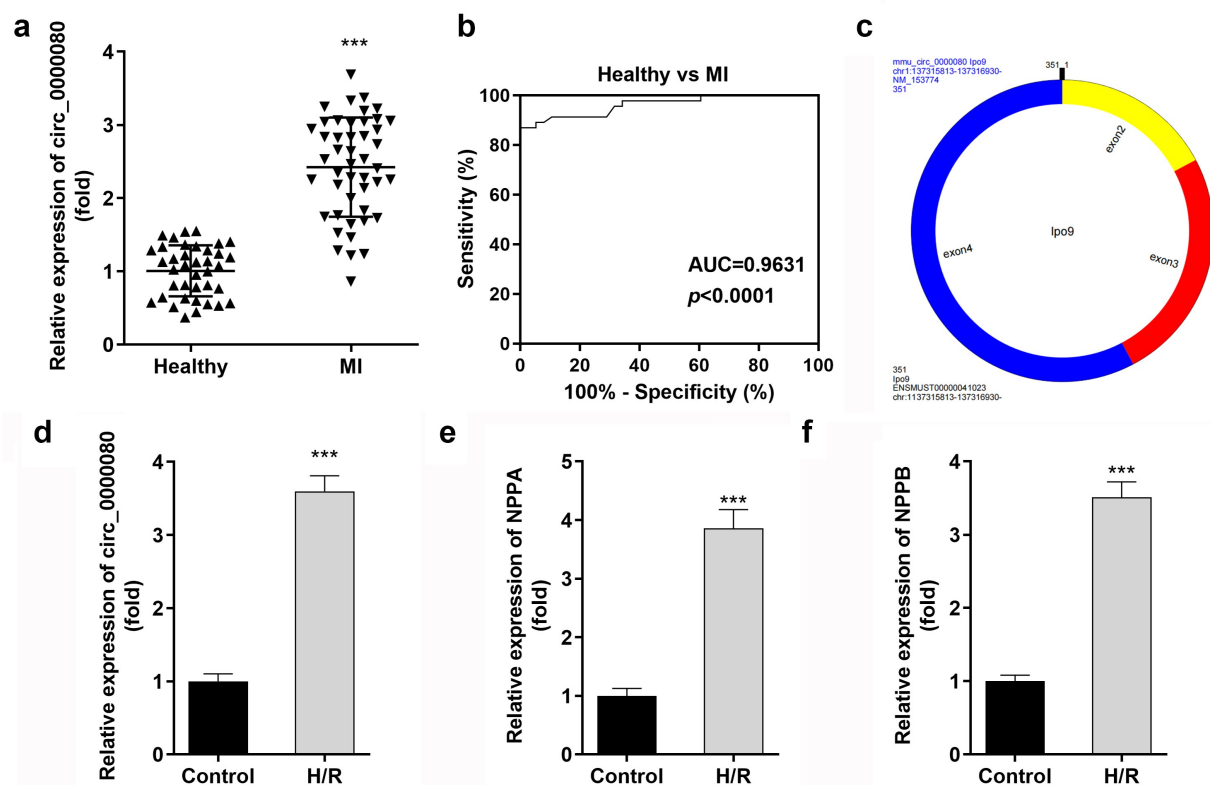


**Figure 1.** Circ\_0000080 is upregulated in patients with MI and in H/R-treated cells. (a) circ\_0000080 was upregulated in patients with MI. (b) ROC analysis for the distinction between patients with MI and healthy controls. (c) The information of circ\_0000080. (d) The circ\_0000080 level was analyzed by qRT-PCR after H/R treatment ( $n = 3$ ). (e) Detection of NPPA expression in H/R cells ( $n = 3$ ). (f) Detection of NPPA expression in H/R cells ( $n = 3$ ). \*\* $p < 0.01$ , \*\*\* $p < 0.001$ .

in H9c2 cells (Figure 1(d)). Moreover, the expression of NPPA and NPPB was upregulated in H/R treated H9c2 cells (Figure 1(e, f)).

### Circ\_0000080 knockdown attenuates hypoxia/reoxygenation-induced injuries in H9c2 cells

The expression level of circ\_0000080 was markedly reduced by si-circ\_0000080 1# compared to si-circ\_0000080 2#, while si-circ\_0000080 1# did not affect the linear GAPDH expression level (Figure 2(a, b)). Such finding suggests that circ\_0000080 is indeed a circular transcript. As shown in Figure 2(c), h/R treatment markedly weakened H9c2 cell viability, which was remarkably improved by circ\_0000080 knockdown. Hypoxia/reoxygenation-induced

apoptotic cell ratio and Bax/Bcl-2 protein ratio were also substantially reduced by circ\_0000080 knockdown in H/R-treated H9c2 cells (Figure 2(d, e)).

### Downregulation of circ\_0000080 suppresses inflammation in H9c2 cells induced by H/R

Inflammation after MI is necessary for heart repair; however, inflammation is also involved in the pathophysiological processes, such as heart remodeling and heart failure after MI [19]. As shown Figure 3, compared to control cells, H/R treatment/exposure significantly increased the release of IL-1 $\beta$ , IL-6, and TNF- $\alpha$ , which was reversed by knockdown of circ\_0000080 (Figure 3(a-c)).

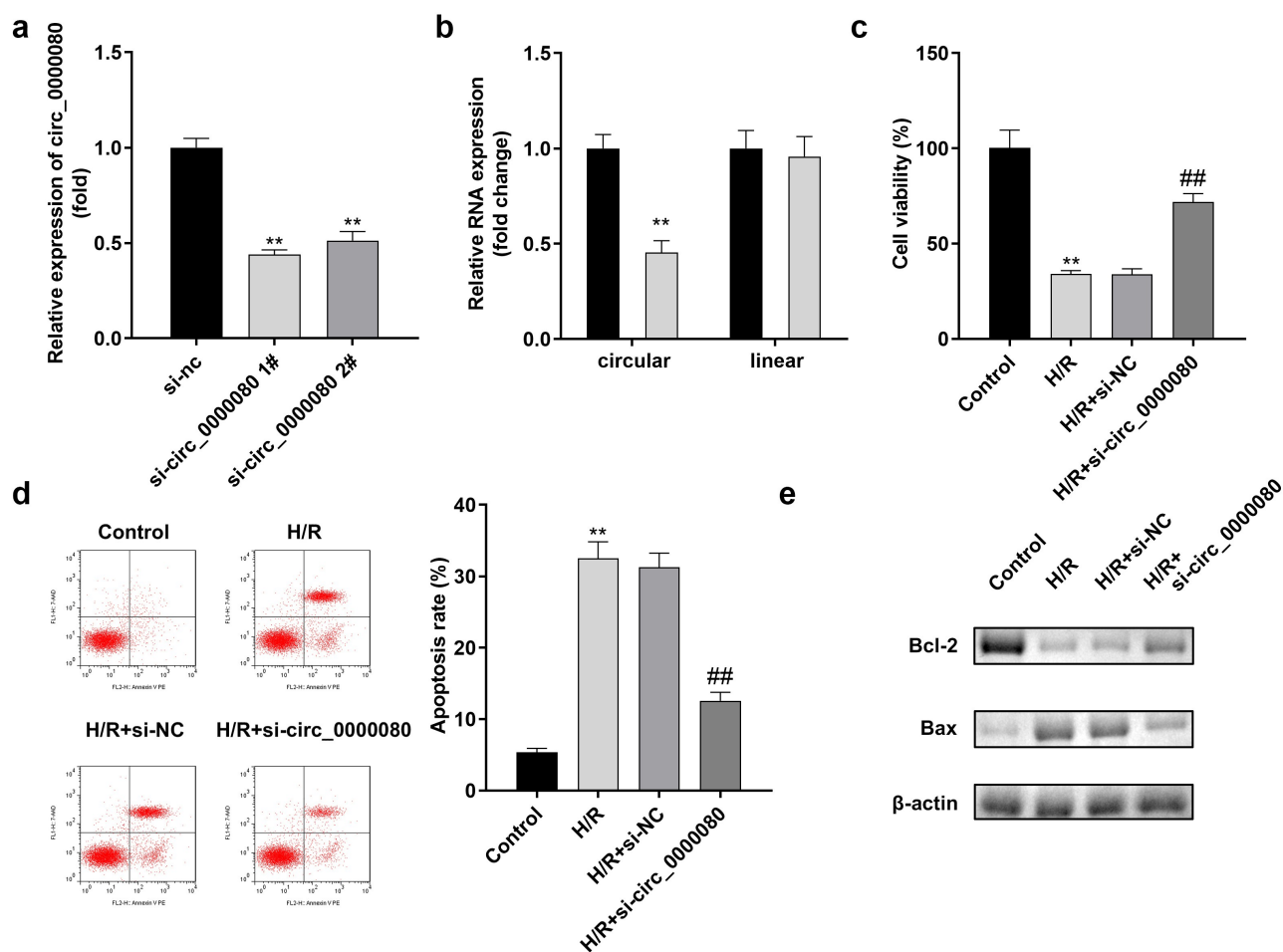


**Figure 2.** Knockdown of circ\_0000080 inhibits H9c2 apoptosis induced by H/R. (a) The expression of circ\_0000080 was down-regulated in H9c2 cells by si-circ\_0000080 1# (n = 3). (b) The circular characteristics of circ\_0000080 was validated (n = 3). (c) Cell viability analysis with CCK-8 (n = 3). (d) Apoptosis analysis (n = 3). (e) Levels of Bcl-2 and Bax were examined by western blotting (n = 3). \*\*p < 0.01, ##p < 0.01.

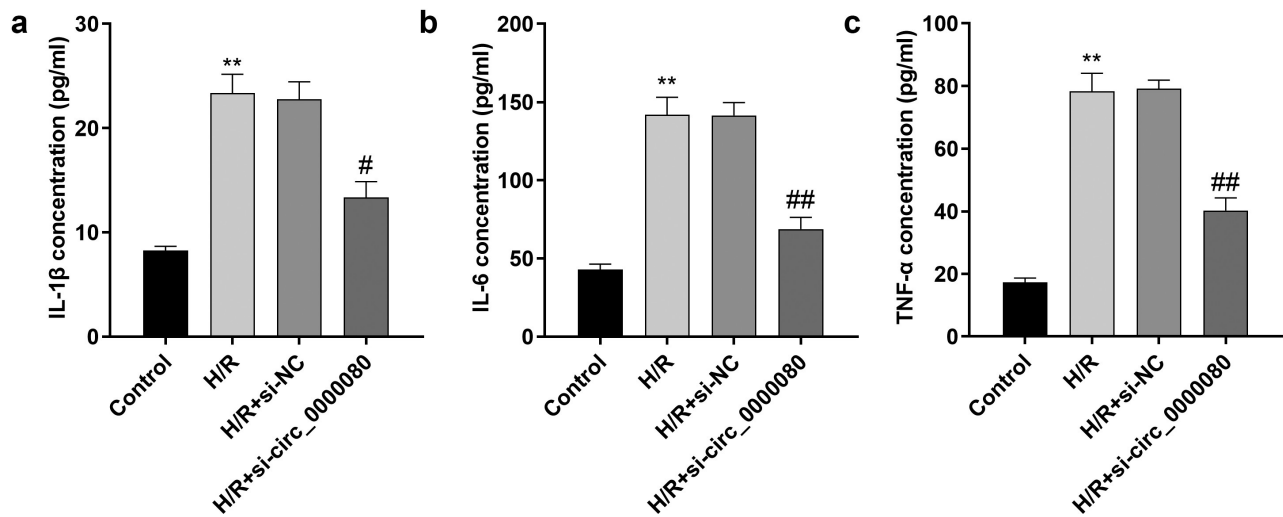


**Figure 3.** Knockdown of circ\_0000080 suppresses H9c2 cell inflammation induced by H/R. (a) The concentration of IL-1 $\beta$  in H9c2 cells (n = 3). (b) The concentration of IL-6 in H9c2 cells (n = 3). (c) The concentration of TNF- $\alpha$  in H9c2 cells (n = 3). \*\*p < 0.01, #p < 0.05, ##p < 0.01.

### Circ\_0000080 targets miR-367-5p in cardiac myocytes

Based on increasing evidence, circRNA acts as a miRNA sponge [20,21]. The binding sites of

circ\_0000080 and miR-367-5p are shown in Figure 4(a). MiR-367-5p mimics significantly down-regulated the luciferase activity of circ\_0000080 3'-UTR-wt in H9c2 cells (Figure 4(b)); however, no

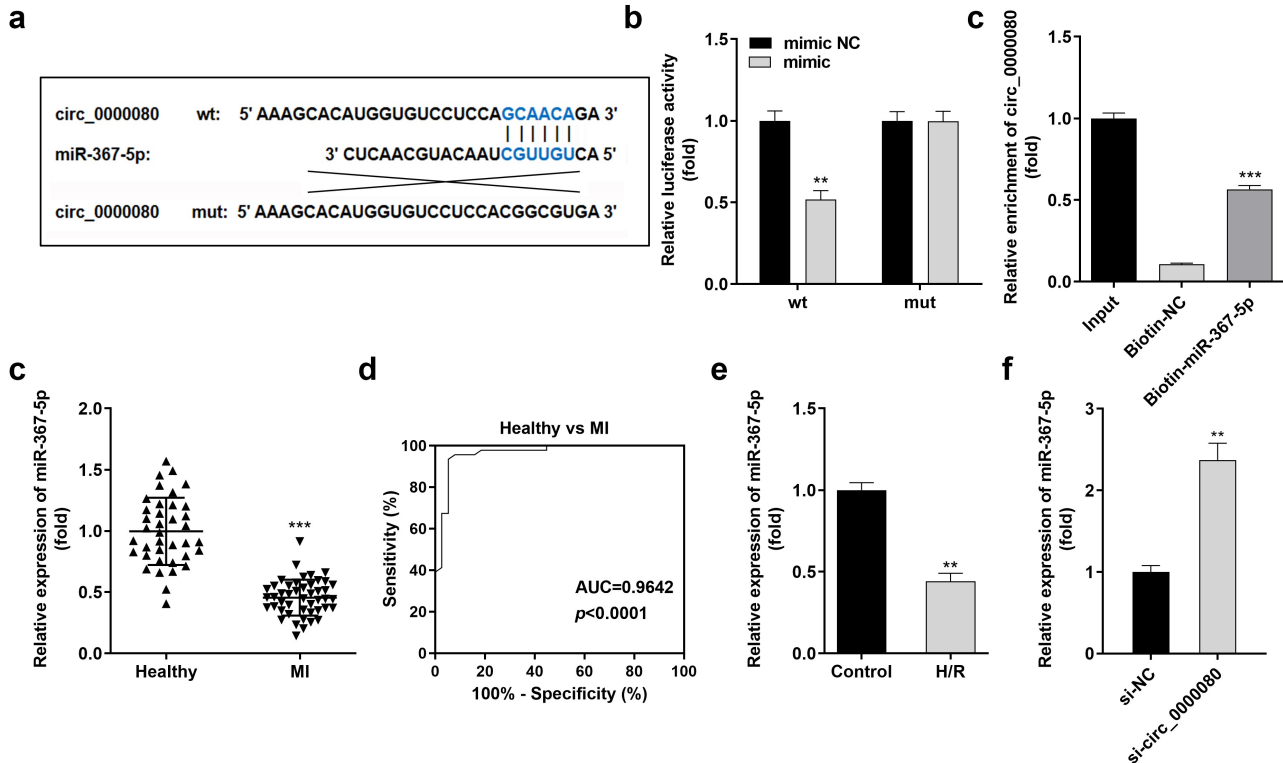


**Figure 4.** MiR-367-5p is a target of circ\_0000080. (a) The binding site between circ\_0000080 and miR-367-5p. (b) Luciferase activity of circ\_0000080 3'-UTR-WT or MuT in H9c2 cells (n = 3). (c) RNA pull-down assay (n = 3). (d) MiR-367-5p was upregulated in patients with MI. (e) ROC analysis for the distinction between patients with MI and healthy controls. (f) The miR-367-5p level was analyzed by qRT-PCR (n = 3). (g) Detection of miR-367-5p expression in H/R cells (n = 3). \*\*p < 0.01, \*\*\*p < 0.001.

obvious changes were found in cells transfected with circ\_0000080 3'-UTR-mut. The results of the RNA pull-down assay suggested that biotin-miR-367-5p could notably pull down more circ\_0000080 (Figure 4(c)). Further, the expression level of miR-367-5p was significantly reduced in MI patients compared to normal controls (Figure 4(d)), and the corresponding AUC value of miR-367-5p for distinguishing between MI patients and healthy controls was 0.9642 (Figure 4(e)). Besides, the expression level of miR-367-5p was remarkably diminished in H/R-treated H9c2 cells (figure 4(f)). The qRT-PCR data revealed that the expression of miR-367-5p was reinforced in H9c2 cells with circ\_0000080 knockdown (Figure 4(g)).

### MiR-367-5p knockdown reverses the effect of circ\_0000080 knockdown in H/R-treated H9c2 cells

A rescue experiment was conducted to explore the relationship between circ\_0000080 and miR-367-5p in H/R treated H9c2 cells. Based on qPCR, the miR-367-5p inhibitor significantly reduced the expression level of miR-367-5p, while the miR-367-5p mimic markedly increased the expression level of miR-367-5p (Figure 5(a)). The CCK-8 assay indicated that circ\_0000080 knockdown reduced the viability of H/R-treated H9c2 cells, which was reversed by the miR-367-5p inhibitor (Figure 5(b)). Further, the miR-367-5p inhibitor alleviated the inhibition of H/R-treated H9c2 apoptosis induced by circ\_0000080 knockdown (Figure 5(c-e)).

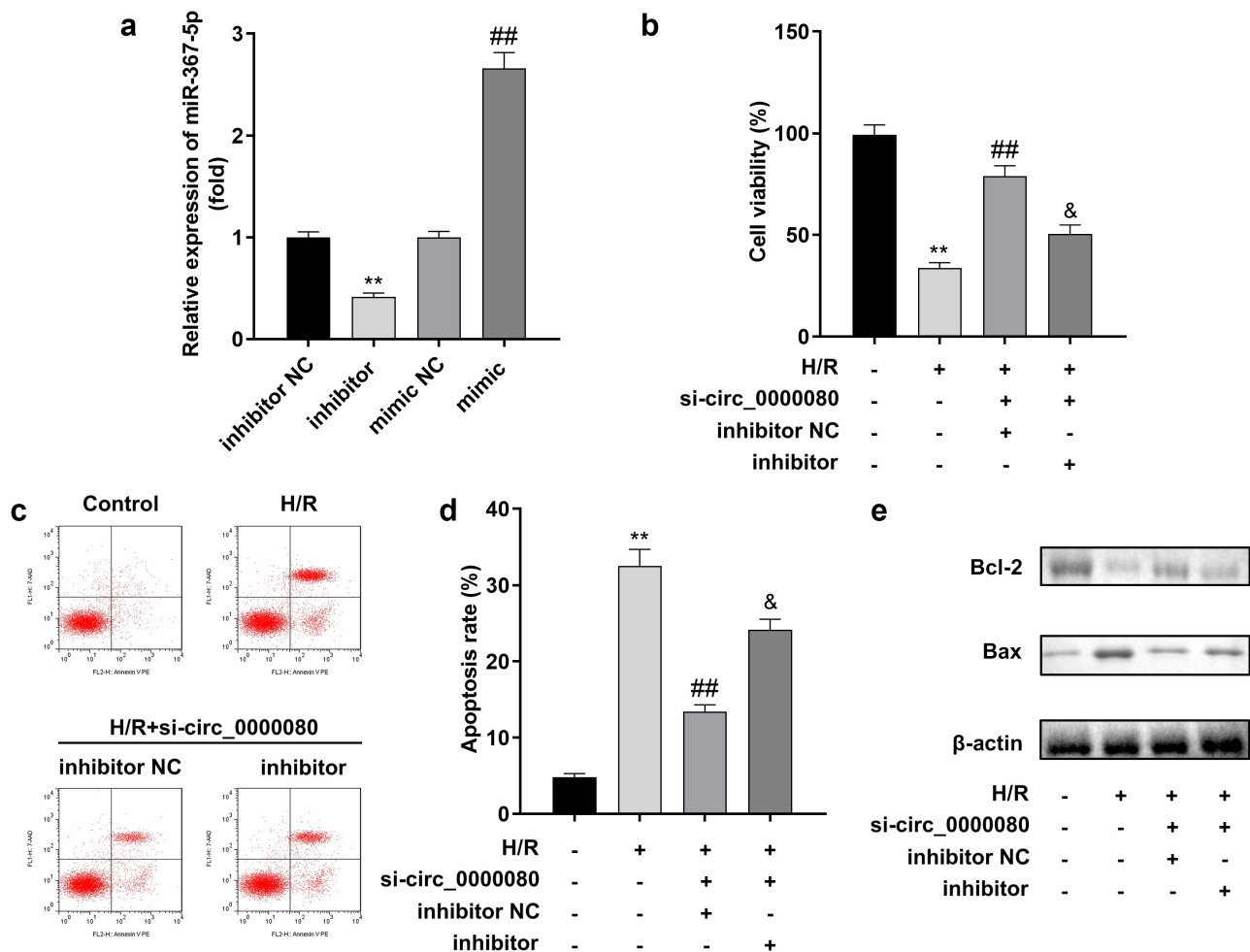


**Figure 5.** MiR-367-5p knockdown reverses the effect of circ\_0000080 on H/R-treated H9c2 cells. (a) The expression of miR-367-5p (n = 3). (b) Cell viability (n = 3). (c-d) Flow cytometry (n = 3). (e) Western blot (n = 3). \*\*p < 0.01, ##p < 0.01.

### Knockdown of miR-367-5p promotes inflammatory response

To determine the effects of miR-367-5p in H/R-treated H9c2 cells, an experiment was conducted to further assess the effects of miR-367-5p on the

secretion of inflammatory factors in H9c2 cells in vitro. Knockdown of circ\_0000080 reduced the release of inflammatory cytokines including IL-1 $\beta$ , IL-6, and TNF- $\alpha$ , and the miR-367-5p inhibitor was found to increase the secretion of IL-1 $\beta$ , IL-6, and TNF- $\alpha$  (Figure 6(a-c)).

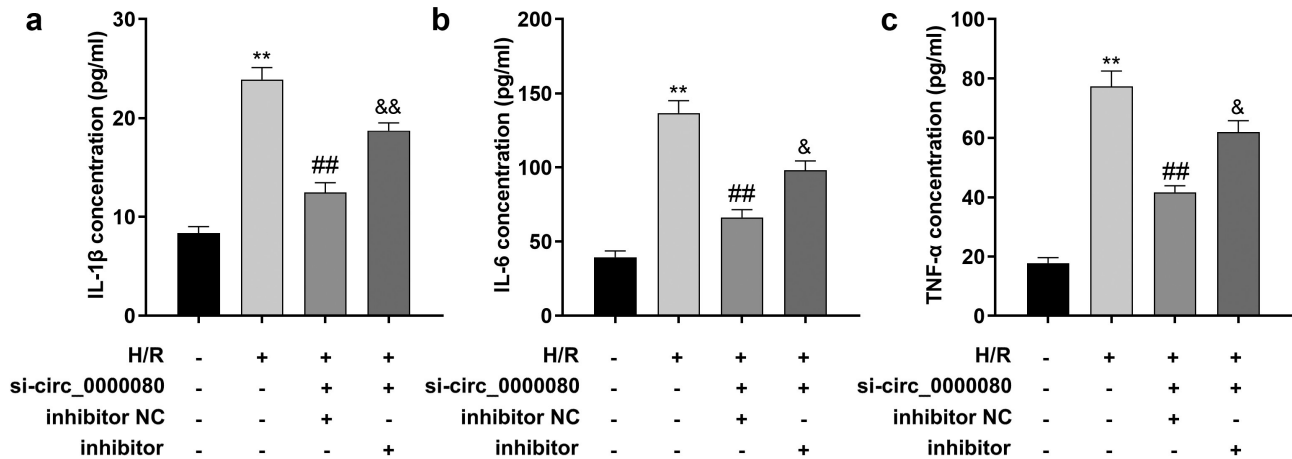


**Figure 6.** Knockdown of miR-367-5p reverses the reduction of inflammatory factors in H/R-treated H9c2 cells induced by circ\_0000080 knockdown. (a) The concentration of IL-1 $\beta$  in H9c2 cells (n = 3). (b) The concentration of IL-6 in H9c2 cells (n = 3). (c) The concentration of TNF- $\alpha$  in H9c2 cells (n = 3). \*\*p < 0.01, ##p < 0.01.

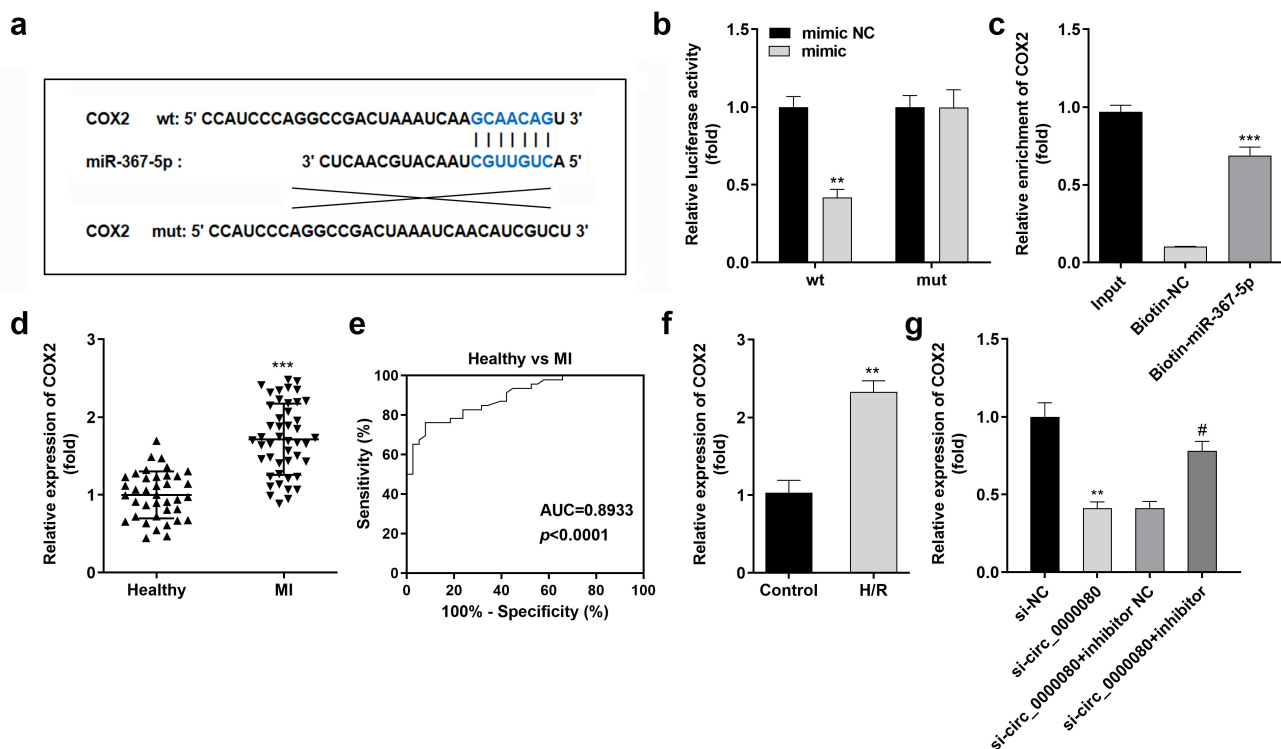


**Figure 7.** MiR-367-5p directly targets COX2 in H9c2 cells. (a) The binding site between COX2 and miR-367-5p. (b) Luciferase activity of COX2 3'-UTR-WT or MuT in H9c2 cells (n = 3). (c) RNA pull-down assay (n = 3). (d) COX2 was upregulated in patients with MI. (e) ROC analysis for the distinction between patients with MI and healthy controls. (f) The COX2 level in H/R-treated H9c2 cells was analyzed by qRT-PCR (n = 3). (g) The relationship among circ\_0000080, miR-367-5p, and COX2 (n = 3). \*\*p < 0.01, \*\*\*p < 0.001, #p < 0.05.



### MiR-367-5p directly targets COX2 in H9c2 cells

The Starbase online software was used to predict the potential target of miR-367-5p to clarify the mechanism of the circ\_0000080/miR-367-5p signaling pathway in MI. The binding sites of miR-367-5p and COX2 are shown in Figure 7(a), and were further verified by the luciferase and RNA pull-down assays (Figure 7(b, c)). MiR-367-5p was found to inhibit the luciferase activity of the reporter carrying COX2-wt. Further, the RNA pull-down assay suggested that biotin-miR-367-5p could notably pull down more circ\_0000080 (Figure 7(c)). The mRNA expression level of COX2 was remarkably elevated in MI patients compared to normal controls (Figure 7(d)), and the corresponding AUC value of miR-367-5p for

distinguishing between MI patients and healthy controls was 0.8933 (Figure 7(e)). Besides, COX2 expression level was significantly elevated in H/R-treated H9c2 cells (figure 7(f)) but was reduced by circ\_0000080 knockdown, with normal levels restored after transfection with the miR-367-5p inhibitor (Figure 7(g)).

### Overexpression of COX2 reverses the effect of miR-367-5p in H/R-treated H9c2 cells

A rescue experiment was performed to confirm the relationship between miR-367-5p and COX2 in H/R-treated H9c2 cells. The transfection efficiency of COX2 is shown in Figure 8(a). The viability of H/R-treated H9c2 cells was markedly

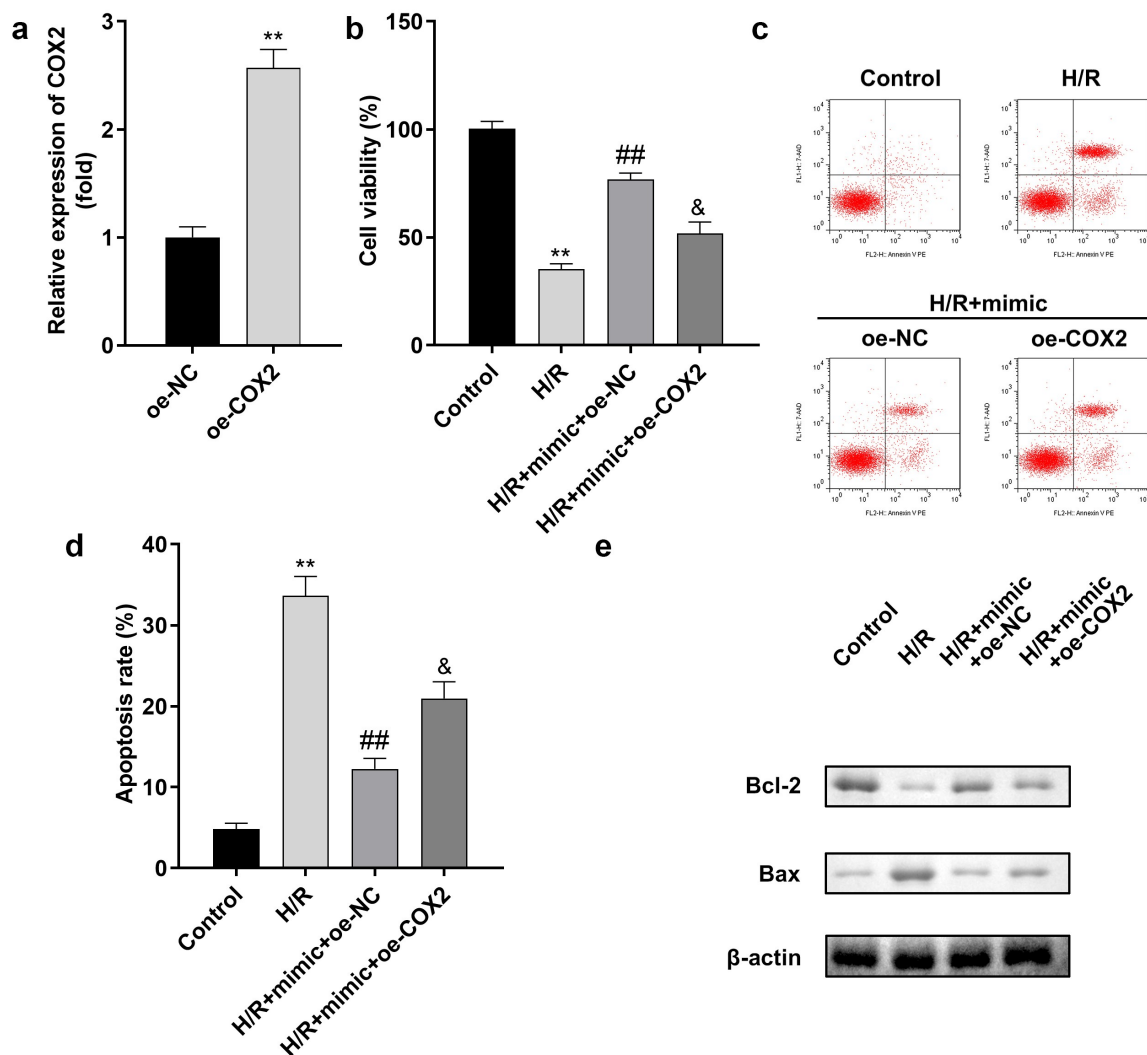


**Figure 8.** Overexpression of COX2 reverses the effect of miR-367-5p in H/R-treated H9c2 cells. (a) The expression of COX2 (n = 3). (b) Cell viability (n = 3). (c-d) Flow cytometry (n = 3). (e) Western blot (n = 3). \*\*p < 0.01, ##p < 0.01.

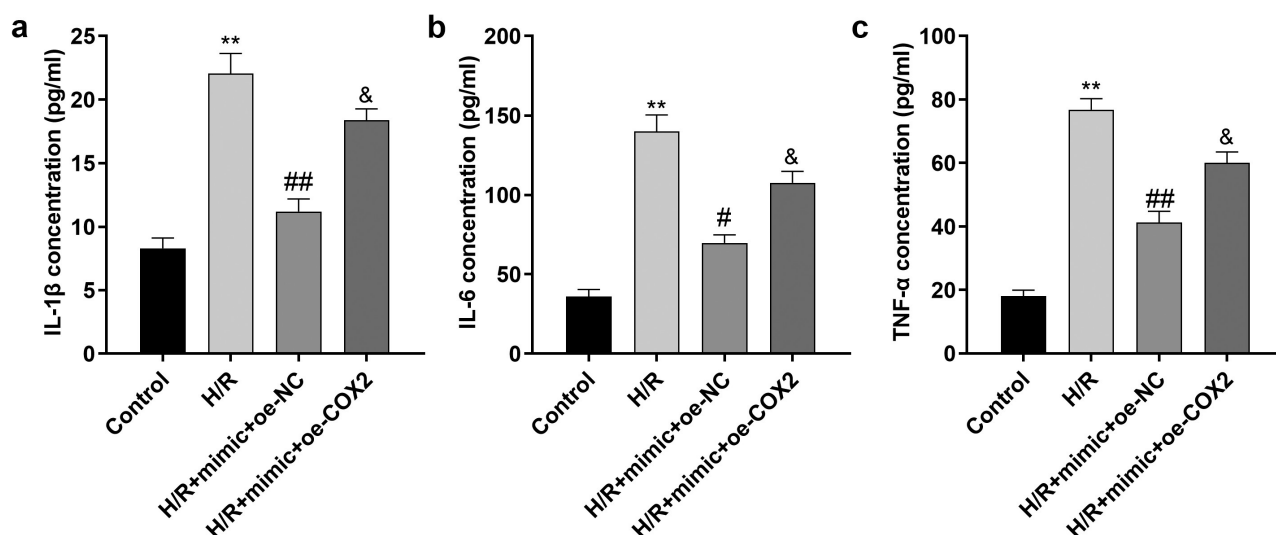


**Figure 9.** Overexpression of *COX2* reverses the reduction of inflammatory factors in H/R-treated H9c2 cells induced by the miR-367-5p mimic. (a) The concentration of IL-1 $\beta$  in H9c2 cells (n = 3). (b) The concentration of IL-6 in H9c2 cells (n = 3). (c) The concentration of TNF- $\alpha$  in H9c2 cells (n = 3). \*\*p < 0.01, #p < 0.05, ##p < 0.01.

improved by the miR-367-5p mimic, which was inhibited by *COX2* overexpression (Figure 8(b)). Moreover, *COX2* overexpression promoted apoptosis in H9c2 cells (Figure 8(c-e)).

#### Overexpression of *COX2* reverses the reduction of inflammatory factors in H/R-treated H9c2 cells induced by the miR-367-5p mimic

The overexpression of *COX2* significantly increased the release of inflammatory cytokines, such as IL-1 $\beta$ , IL-6, and TNF- $\alpha$ , as shown in Figure 9.

#### Discussion

The cardiovascular system is the engine of life. Severe cardiovascular disease is a potentially fatal disease [22,23]. Although the standards for the prevention, diagnosis, and treatment of such diseases have significantly improved, the mortality rate associated with MI is still high [24]. Understanding the regulatory mechanism post-H/R injury is essential to improve the prognosis and treatment of MI. To our knowledge, this is the first study to reveal that circ\_0000080 is upregulated in MI patients and in H/R-treated H9c2 cells. Moreover, the knockdown of circ\_0000080 reduced the rate of apoptosis and inhibited inflammation induced by H/R. circ\_0000080 targeted

miR-367-5p in cardiomyocytes and miR-367-5p targeted *COX2*. MiR-367-5p knockdown or *COX2* overexpression inhibited the role of circ\_0000080 in MI.

Apoptosis is a form of programmed cell death; it affects cardiomyocytes during MI [25]. The increase in the extent of hypoxia caused by blood flow interruption and the increase in the level of oxidative stress during ischemia-reperfusion can lead to myocardial apoptosis [26]. H/R-induced apoptosis and inflammatory response are two key factors in the progression of H/R-induced heart injury. Myocardial cells have low regenerative ability; thus, reducing their level of apoptosis and inhibiting inflammatory response in these cells can help protect a patient's heart function and improve the prognosis [27]. CircRNAs play crucial roles in cardiac pathophysiological changes during heart failure. For example, the expression level of circ ACAP2 is upregulated in MI patients and it promotes apoptosis by binding to miR-29 [28]. Knockdown of circ\_0060745 alleviates MI by inhibiting myocardial apoptosis and inflammation [29]. However, the regulatory role of circRNA in cardiomyocyte apoptosis is still unclear. Here, we studied the expression of circ\_0000080 in MI patients and healthy controls – circ\_0000080 was upregulated in MI patients and similarly upregulated in H/R treated H9c2 cells. To investigate the

function of circ\_0000080 in H9c2 cells, we sought to determine the effect of circ\_0000080 on the viability of H9c2 cells. circ\_0000080 knockdown was found to attenuate hypoxia/reoxygenation-induced injuries of H9c2 cells and suppress inflammation in cells. These results suggest that circ\_0000080 inhibition can improve the function of cardiomyocytes by inhibiting apoptosis and decreasing the expression levels of inflammatory factors.

We proceeded to explore the mechanism of circ\_0000080 in MI. Most circRNAs play regulatory roles in MI by targeting downstream genes [30,31]. Liu et al. found that circYAP1 binds to miR-367-5p and antagonizes the downregulation of p27 Kip1 by miR-367-5p, thereby inhibiting the proliferation and invasion of GC cells [32]. Accordingly, miR-367-5p was first predicted and identified as a novel downstream miRNA target of circ\_0000080 in cardiomyocytes. In this study, miR-367-5p was found to be significantly down-regulated in MI patients and H/R-treated H9c2 cells. Moreover, miR-367-5p knockdown reversed the effect of circ\_0000080 and the reduction of inflammatory factors in cells. We revealed, for the first time, the function of miR-367-5p in MI and proved that miR-367-5p was targeted by circ\_0000080 to regulate H/R damage.

To further study the mechanism of miR-367-5p's biological function in MI, we investigated the downstream target gene of miR-367-5p. Zhang et al. found that COX2 knockdown may increase the risk of MI [32]. Herein, miR-367-5p was found to directly target COX2 in H9c2 cells, and the overexpression of COX2 reversed the effect of miR-367-5p in cells. Therefore, circ\_0000080 may weaken the targeted inhibitory effect of miR-367-5p on COX2 by binding to miR-367-5p, thereby inhibiting the progression of MI. The circ\_0000080/miR-367-5p/COX2 axis may provide a new therapeutic option for MI.

The main limitation of this study is that the role of the circ\_0000080/miR-367-5p/COX2 axis in MI needs to be confirmed using several clinical studies, which will be the focus and a challenge of future research. Additionally, only the roles of miR-367-5p and COX2 were explored in this study. Whether other miRNAs and genes influence circ\_0000080-mediated regulation in MI still needs to be elucidated.

## Conclusion

In summary, the circ\_0000080/miR-367-5p/COX2 signal axis was found to promote proliferation and impair the apoptosis of H/R treated cells. This study not only revealed the novel roles of the circ\_0000080/miR-367-5p/COX2 axis in MI, but also provided a new target for the management of MI.

## Authors' contributions

All authors participated in the design, interpretation of the studies and analysis of the data and review of the manuscript. B W drafted the work and revised it critically for important intellectual content; YY Z and SM F were responsible for the acquisition, analysis, or interpretation of data for the work; H W made substantial contributions to the conception or design of the work.

## Disclosure statement

No potential conflict of interest was reported by the author(s).

## Funding

The author(s) reported there is no funding associated with the work featured in this article.

## Data availability

The datasets used and analyzed during the current study are available from the corresponding author on reasonable request.

## References

- [1] Lu L, Liu M, Sun R, et al. Myocardial infarction: symptoms and treatments. *Cell Biochem Biophys*. 2015;72(3):865–867.
- [2] de Lemos JA, Newby LK, Mills NL, et al. A proposal for modest revision of the definition of type 1 and type 2 myocardial infarction. *Circulation*. 2019;140(22):1773–1775.
- [3] Krishnaswami A, Maurer MS, Alexander KP. Contextualizing myocardial infarction: comorbidities and priorities in older adults. *Am J Med*. 2017;130(10):1144–1147.
- [4] Velibey Y, Erbay A, Ozkurt E, et al. Acute myocardial infarction associated with blood transfusion: case report and literature review. *Transfus Apher Sci*. 2014;50(2):260–262.

- [5] Nikulina NN, Yakushin SS. The modern aspects of diagnosis formulation and statistical recording of myocardial infarction. *Kardiologija*. 2016;56:60–66.
- [6] Jin J, Sun H, Shi C, et al. Circular RNA in renal diseases. *J Cell Mol Med*. 2020;24(12):6523–6533.
- [7] Altesha MA, Ni T, Khan A, et al. Circular RNA in cardiovascular disease. *J Cell Physiol*. 2019;234(5):5588–5600.
- [8] Lu D, Thum T. RNA-based diagnostic and therapeutic strategies for cardiovascular disease. *Nat Rev Cardiol*. 2019;16(11):661–674.
- [9] Hsiao KY, Sun HS, Tsai SJ. Circular RNA - new member of noncoding RNA with novel functions. *Exp Biol Med*. 2017;242(11):1136–1141.
- [10] Garikipati VNS, Verma SK, Cheng Z, et al. Circular RNA circfndc3b modulates cardiac repair after myocardial infarction via fus/vegf- $\alpha$  axis. *Nat Commun*. 2019;10(1):4317.
- [11] Zeng Z, Xia L, Fan S, et al. Tang WH: circular RNA circmap3k5 acts as a miRNA-22-3p sponge to promote resolution of intimal hyperplasia via tet2-mediated smooth muscle cell differentiation. *Circulation*. 2021;143(4):354–371.
- [12] Li H, Xu JD, Fang XH, et al. Circular RNA circrna\_000203 aggravates cardiac hypertrophy via suppressing mir-26b-5p and mir-140-3p binding to gata4. *Cardiovasc Res*. 2020;116(7):1323–1334.
- [13] Mohr AM, Mott JL. Overview of miRNA biology. *Semin Liver Dis*. 2015;35(1):3–11.
- [14] Zhang L, Liao Y, Tang L. MiRNA-34 family: a potential tumor suppressor and therapeutic candidate in cancer. *J Exp Clin Cancer Res*. 2019;38(1):53.
- [15] Gu Y, Zhang Y, Zhao C, et al. Serum miRNAs as potential biomarkers of mandibular prognathism. *Oral Dis*. 2014;20(1):55–61.
- [16] Liu H, Liu Y, Bian Z, et al. Circular RNA yap1 inhibits the proliferation and invasion of gastric cancer cells by regulating the mir-367-5p/p27 (kip1) axis. *Mol Cancer*. 2018;17(1):151.
- [17] Jin L, Zhang Y, Jiang Y, et al. Circular RNA Rbms1 inhibited the development of myocardial ischemia reperfusion injury by regulating miR-92a/BCL2L1 signaling pathway. *Bioengineered*. 2022;13(2):3082–3092.
- [18] Fang L, Xu X, Lu Y, et al. Long noncoding RNA SNHG8 accelerates acute gouty arthritis development by upregulating AP3D1 in mice. *Bioengineered*. 2021;12(2):9803–9815.
- [19] Prabhu SD, Frangogiannis NG. The biological basis for cardiac repair after myocardial infarction: from inflammation to fibrosis. *Circ Res*. 2016;119(1):91–112.
- [20] Xiao L, Wang W, Zhao J, et al. LncRNA malat1 promotes cell proliferation and invasion by regulating the mir-101/ezh2 axis in oral squamous cell carcinoma. *Oncol Lett*. 2020;20(5):164.
- [21] Wang L, Song H, Yang S. MicroRNA-206 has a bright application prospect in the diagnosis of cases with oral cancer. *J Cell Mol Med*. 2021;25(17):8169–8173.
- [22] Francula-Zaninovic S, Nola IA. Management of measurable variable cardiovascular disease' risk factors. *Curr Cardiol Rev*. 2018;14(3):153–163.
- [23] Leong DP, Joseph PG, McKee M, et al. Reducing the global burden of cardiovascular disease, part 2: prevention and treatment of cardiovascular disease. *Circ Res*. 2017;121(6):695–710.
- [24] Zhao D, Liu J, Wang M, et al. Epidemiology of cardiovascular disease in China: current features and implications. *Nat Rev Cardiol*. 2019;16(4):203–212.
- [25] Aymong ED, Ramanathan K, Buller CE. Pathophysiology of cardiogenic shock complicating acute myocardial infarction. *Med Clin North Am*. 2007;91(4):701–712. xii.
- [26] Yoshimura C, Nagasaka A, Kurose H, et al. Efferocytosis during myocardial infarction. *J Biochem*. 2020;168(1):1–6.
- [27] Luo KQ, Long HB, Xu BC. Reduced apoptosis after acute myocardial infarction by simvastatin. *Cell Biochem Biophys*. 2015;71(2):735–740.
- [28] Liu X, Wang M, Li Q, et al. CircRNA acap2 induces myocardial apoptosis after myocardial infarction by sponging mir-29. *Minerva Med*. 2020;113(1):128–134.
- [29] Zhai C, Qian G, Wu H, et al. Knockdown of circ\_0060745 alleviates acute myocardial infarction by suppressing nf-kappaB activation. *J Cell Mol Med*. 2020;24(21):12401–12410.
- [30] Pan G, Mao A, Liu J, et al. Circular RNA hsa\_circ\_0061825 (circ-tff1) contributes to breast cancer progression through targeting mir-326/tff1 signalling. *Cell Prolif*. 2020;53(2):e12720.
- [31] Lei B, Huang Y, Zhou Z, et al. Circular RNA hsa\_circ\_0076248 promotes oncogenesis of glioma by sponging mir-181a to modulate sirt1 expression. *J Cell Biochem*. 2019;120(4):6698–6708.
- [32] Zhang L, Deng M, Lu A, et al. Sodium butyrate attenuates angiotensin II-induced cardiac hypertrophy by inhibiting COX2/pge2 pathway via a hdac5/hdac6-dependent mechanism. *J Cell Mol Med*. 2019; 23(12):8139–8150.